Journal of Materials Chemistry A

Wide-bandgap polymer based on alkylphenyl-substituted benzo[1,2-b:4,5-b']dithiophene unit with high power conversion efficiency of over 11%

Journal:	*Journal of Materials Chemistry A*
Manuscript ID	TA-ART-06-2018-005868.R1
Article Type:	Paper
Date Submitted by the Author:	27-Jul-2018
Complete List of Authors:	Guo, Xia; Soochow University, Laboratory of Advanced Optoelectronic Materials, College of Chemistry, Chemical Engineering and Materials Science Li, Wanbin; Soochow University, College of Chemistry, Chemical Engineering and Materials Science Guo, Huan; Xiangtan University, College of Chemistry Guo, Bing; Soochow University, College of Chemistry, Chemical Engineering and Materials Science Wu, Jingnan ; Soochow University, Laboratory of Advanced Optoelectronic Materials, College of Chemistry, Chemical Engineering and Materials Science Ma, Wei; Xi'an Jiaotong University, State Key Laboratory for Mechanical Behavior of Materials Zhang, Maojie; Soochow University, Laboratory of Advanced Optoelectronic Materials, College of Chemistry, Chemical Engineering and Materials Science Wong, Wai-Yeung (Raymond); The Hong Kong Polytechnic University, Faculty of Applied Science and Textiles

Wide-bandgap polymer based on alkylphenyl-substituted benzo[1,2-*b*:4,5-*b'*]dithiophene unit with high power conversion efficiency of over 11%

Xia Guo, Wanbin Li, Huan Guo, Bing Guo, Jingnan Wu, Wei Ma, Maojie Zhang, Wai-Yeung Wong**

Dr. X. Guo, W. B. Li, H. Guo, B. Guo, J. N. Wu, Prof. M. J. Zhang
Laboratory of Advanced Optoelectronic Materials, College of Chemistry, Chemical Engineering and Materials Science, Soochow University, Suzhou 215123, China
*E-mail: mjzhang@suda.edu.cn
Dr. X. Guo, Prof. W.-Y. Wong
Institute of Molecular Functional Materials and Department of Applied Biology and Chemical Technology, The Hong Kong Polytechnic University, Hung Hom, Hong Kong, China
*E-mail: wai-yeung.wong@polyu.edu.hk
Prof. W. Ma
State Key Laboratory for Mechanical Behavior of Materials, Xi'an Jiaotong University, Xi'an 710049, China

Abstract

A novel wide-bandgap conjugated polymer (PTZP) based on alkylphenyl-substituted benzo[1,2-*b*:4,5-*b'*]dithiophene (BDT-P) as electron-rich unit and thiazolo[5,4-*d*]thiazole (TTz) as electron-deficient unit was designed and synthesized for non-fullerene polymer solar cells (PSCs) application. The polymer exhibits a wide bandgap of 2.01 eV with strong absorption in the range of 300-620 nm, which is complementary with that of fused-ring small molecule acceptor (SMA) 2,2'-((2*Z*,2'*Z*)-((4,4,9,9-tetrahexyl-4,9-dihydro-s-indaceno[1,2-*b*:5,6-*b*']dithiophene-2,7-diyl)bis(methanylylidene))bis(3-oxo-2,3-dihydro-1*H*-indene-2,1-diylidene))dimalononitrile (IDIC), and a deep highest occupied molecular orbital (HOMO) energy level of -5.41 eV. Furthermore, the polymer film possesses strong crystallinity and a

dominated face on stacking with a small d-spacing of 3.65 Å, resulting in a high hole mobility of 4.01×10^{-3} cm^2 V^{-1} s^{-1}. The optimal PSCs based on the PTZP:IDIC blend show a high PCE of 11.8%, with an open-circuit voltage (V_{oc}) of 0.90 V, a short-circuit current density (J_{sc}) of 17.9 mA cm^{-2} and a fill factor (FF) of 73.3%. Meanwhile, the devices also exhibit outstanding performance with PCE over 10% with the active layer thickness of up to 200 nm or the area of up to 0.81 cm^2, resulting from the excellent molecular stacking. These results reveal that the PTZP will be a promising conjugated polymer for the fabrication of efficient large-area PSCs.

Keywords: non-fullerene polymer solar cells, alkylphenyl-substituted benzo[1,2-*b*:4,5-*b'*]dithiophene, thiazolo[5,4-*d*]thiazole, high power conversion efficiency, wide bandgap polymer

1. Introduction

Bulk-heterojunction polymer solar cells (BHJ-PSCs) have attracted great attention because of its solution processibility, ease of fabrication, promising flexibility, and low-cost production.[1-10] State-of-the-art power conversion efficiency (PCE) has exceeded 13% for single-junction PSCs by using the wide-bandgap polymer as donor material and non-fullerene (NF) small molecules as acceptor material.[11] Compared with fullerene derivative, NF acceptors with particular advantages such as wide and efficient absorption within 600-800 nm, more finely tuned energy levels and facile synthesis.[12] Since Zhan et. al. reported a novel electron acceptor 3,9-bis(2-methylene-(3-(1,1-dicyanomethylene)-indanone)-5,5,11,11-tetrakis(4-hexyl

phenyl)-dithieno[2,3-*d*:2′,3′-*d*′]-sindaceno[1,2-*b*:5,6-*b*′]-dithiophene (ITIC),[13] uncountable highly efficient NF acceptors such as IDIC,[14] 2,2′-((2*Z*,2′*Z*)-((5,5′-(4,4,9,9-tetrakis(4-hexylphenyl)-4,9-dihydro-s-indaceno-[1,2-*b*:5,6-*b*′]dithiophene-2,7-diyl)bis(4-(2-ethylhexyl)-thiophene-5,2-diyl))bis(methanylylidene))-bis(3-oxo-2,3-dihydro-1H-indene-2,1-diylidene))dimalononitrile (IEIC),[15] and NFBDT,[16] have been synthesized and the PCEs of over 12% have been achieved.[17,18] In order to widen the range of light absorption of the active layer blend film to further improve the efficiency of NF PSCs, it is also necessary to develop new wide-bandgap (WBG) polymer donor materials, which possess well complementary absorption and matched energy levels with the low-bandgap small molecular acceptors.[19-28]

Among the various WBG polymers, the thiazolo[5,4-d]thiazole (TTz) based polymers exhibit excellent performance, due to the rigid and planar structure and weak electron-withdrawing nature of TTz unit.[29] In our previous work, we synthesized a WBG conjugated polymer (named PTZ1) based on TTz as the acceptor unit. By using IDIC as the acceptor material, a high PCE of 11.5% has been obtained,[6] which means that the TTz unit has a huge potential for high photovoltaic performance NF PSCs. But the TTz based polymer is still seldom applied to the NF system until now. Benzo[1,2-*b*:4,5-*b*′]dithiophene (BDT) is one of the most successful electron-rich donor units, as its inherent structural symmetry and rigid fused aromatic system are able to enhance electron delocalization and improve charge mobility.[30-38] Since Yang and Hou et al. introduced 2,4-dioctylthienyl substituents onto the BDT unit and constructed the first polymer based on 2D-conjugated BDT units,[39] various

conjugated side groups, including alkylthienyl,[40-43] alkylphenyl,[44-47] and alkylfuran[48-51] have been introduced in the BDT units. Among them, alkylphenyl substituted BDT (BDT-P) units exhibited their superiority, such as the deep HOMO level and high hole mobility. Hence, the polymers based on TTz and BDT-P show great potential in NF-based polymer solar cell application.

In this work, we designed and synthesized a novel conjugated polymer (PTZP) based on alkylphenyl-substituted BDT (BDTP) as electron-rich unit and TTz as electron-deficient unit (Fig. 1a). The optical, electrochemical, hole mobility, and photovoltaic properties were investigated. By combining the BDTP and TTz, the polymer exhibits a strong absorption spectrum in the visible spectrum (300-620 nm) with a bandgap of 2.01 eV, a deep HOMO energy level of -5.41 eV and an extraordinarily high hole mobility of 4.01×10^{-3} cm^2 V^{-1} s^{-1} (Table S4 in the Supporting Information). By using PTZP as the donor material and IDIC as the acceptor material, non-fullerene PSCs achieved a high PCE of 9.9% for the as-cast film. After optimization by adding 0.75% 1,8-diiodooctane (DIO), the PSCs gave a higher PCE of 11.8% with an open-circuit voltage (V_{oc}) of 0.90 V, a short-circuit current density (J_{sc}) of 17.9 mA/cm^2 and a fill factor (FF) of 73.3%. Fig. 1d lists the correlation of high PCE versus optical bandgap (E_g^{opt}) of polymer obtained in this work and the other literature reports, and the details and related literature information are shown in Table S1 and references in the supporting information, respectively. Obviously, most of the wide-bandgap polymers are obtained with a $E_g^{opt} < 1.9$ eV, and only a few of polymers show $E_g^{opt} > 2.0$ eV and still exhibit high photovoltaic performance.

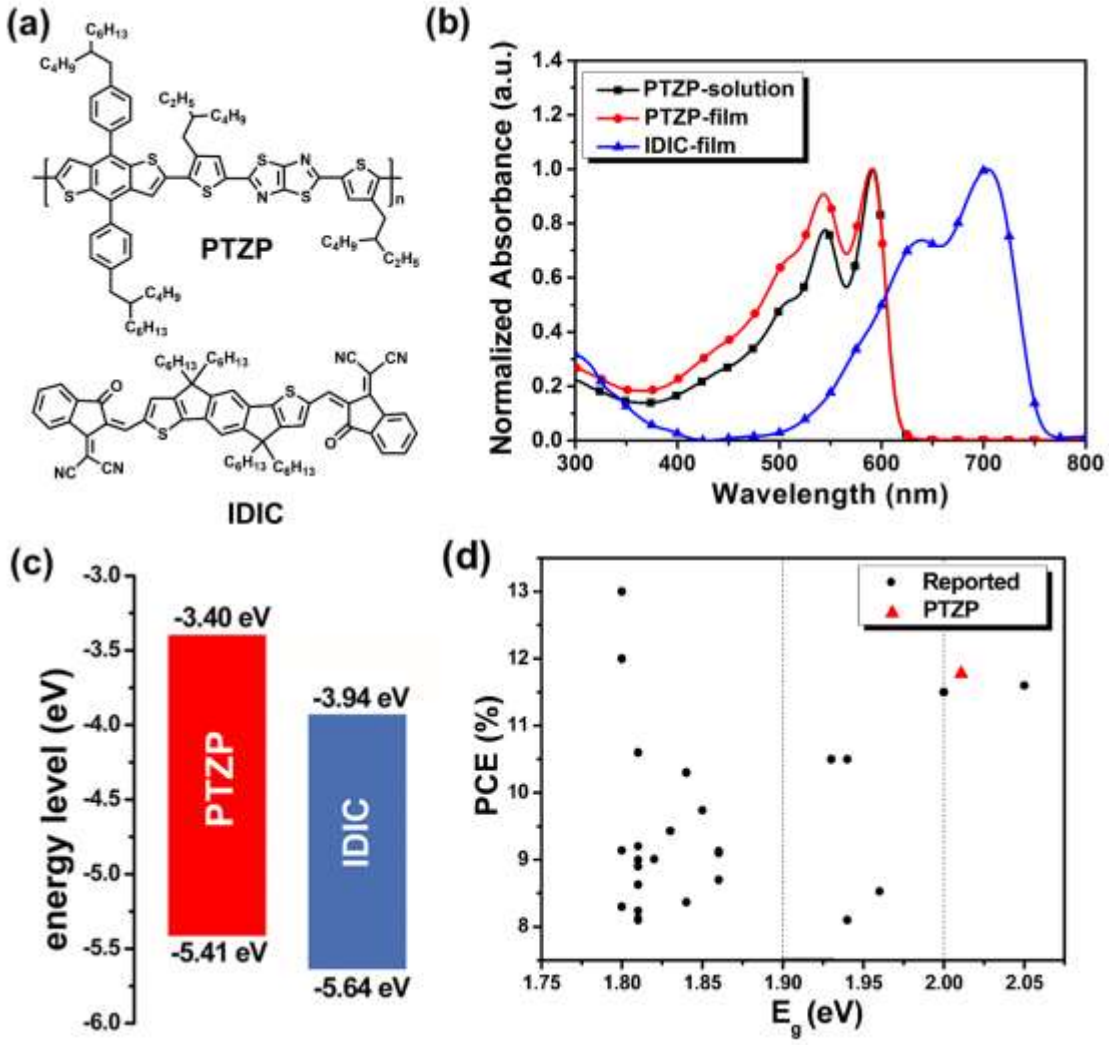

Fig. 1. (a) Chemical structures of PTZP and IDIC, (b) absorption spectra of PTZP and IDIC in thin film, (c) energy level diagram of PTZP and IDIC and (d) the plots of PCE *versus* E_g^{opt}. The dotted lines are the lines of E_g^{opt} at 1.90 eV and 2.00 eV.

2. Results and Discussion

The synthetic route for PTZP is shown in Figure S1 in the Supporting Information. Monomers BDTP[44] and TTz[52] were synthesized according to the previously reported literature references. As shown in Fig. S1, PTZP was synthesized via a typical Stille-coupling reaction using $Pd(PPh_3)_4$ as catalyst and toluene as solvent. High temperature GPC analysis of PTZP afforded the number average molecular weight

(M_n) of 31.33 kDa with a polydispersity index (PDI) of 1.69. Thermogravimetric analysis (TGA) revealed that the decomposition temperature (T_d) with 5% weight-loss is 410 °C (Fig. S2 in the Supporting Information), which means that PTZP has sufficiently good thermal stability for application in PSCs.

The UV-vis absorption spectra of the polymer PTZP in CB solution at different temperatures and in solid film are shown in Figs. 1a and S3. In solution, the absorption intensity of the shoulder peak gradually decreases with the temperature increasing from 20 to 100 ^{o}C, which indicates that PTZP can form strong and stable intermolecular aggregation in low-temperature solutions [53]. In thin film, PTZP shows enhanced vibronic absorption peak and broader absorption in comparison to those in solution. The corresponding optical bandgap (E_g^{opt}) deduced from its absorption edge is estimated to be 2.01 eV. Furthermore, the PTZP: IDIC blend films show the well complementary absorption spectrum from 300 to 800 nm.

With the increasing PCE of PSCs, researchers are paying an increasing attention to the device stability. So far, it is inevitable that the photo-stabilities of the polymers should be addressed due to their influence on the stability of the PSCs.[54-57] To investigate the photo-stabilities of the polymer, we inspected the photo-stabilities of PTZP by exposing the polymers' film with thickness of around 50 nm under AM 1.5 sunlight irradiation in air (Fig. S4a in ESI). The maximal absorption peaks at around 538 and 584 nm for PTZP were gradually decreased as the exposure times were prolonged. After 12 h of irradiation, the PTZP maintained 88.5% of its initial light absorption at the maximal absorption peaks. In addition, the photo-stabilities of PTZP

in film under the 365 nm UV light irradiation in air were also investigated (Fig. S4b). It was shown that PTZP maintained 92.3% of its initial light absorption at the maximal absorption peaks after exposing 12 h of irradiation. It could be found that the PTZP exhibited excellent photo-stability in solid state.

The electrochemical property of PTZP was obtained from cyclic voltammetry (CV) test. As shown in Fig. S5 in the ESI, the onset oxidation potential (φ_{ox}) of PTZP was 0.68 V. The CV curve was recorded versus the potential of a standard $Ag/AgNO_3$ electrode, which was calibrated by the ferrocene-ferrocenium (Fc/Fc^+) redox couple. Under exactly the same conditions, the $\varphi_{1/2}$ of the Fc/Fc^+ redox couple was found to be 0.07 V relative to $Ag/AgNO_3$ reference electrode. Assuming that the redox potential of Fc/Fc^+ was 4.8 eV relative to the vacuum energy level, according to the equation, HOMO = -e (φ_{ox} + 4.73) (eV), the HOMO energy level of PTZP was determined to be -5.41 eV.[58] The LUMO energy level was -3.40 eV as calculated from the HOMO energy level and E_g^{opt}.

The photovoltaic properties of PTZP were investigated by fabricating the PSC devices with a structure of ITO/PEDOT:PSS/PTZP:IDIC/PFN-Br/Al. The detailed optimization processes of the devices for D/A ratios are recorded in Fig. S6 (a) and Table S2 in the Supporting Information, and the different additive contents are shown in Fig. S6a and Table S3 in the Supporting Information. The current density-voltage (*J-V*) curves of the PSCs based on the PTZP:IDIC (1:1.5, w/w) processed with chlorobenzene (CB) as solvent without or with 0.75% DIO are shown in Fig. 2a, and the corresponding photovoltaic parameters are summarized in Table 1. The devices of

as-cast film show a high PCE of 9.9% with a V_{oc} of 0.92 V, a J_{sc} of 16.4 mA cm^{-2}, and a FF of 65.5%. Furthermore, after adding 0.75% DIO, the PCE was increased to 11.8%, due to the further increase of J_{sc} from 16.4 mA cm^{-2} to 17.9 mA cm^{-2} and a sharp increase of FF from 65.5% to 73.3%, which is the highest PCE among the devices based on alkylphenyl-substituted BDT or TTz copolymer as the donor material.

The external quantum efficiency (EQE) curves of all the devices cover a broad photo-response in the wavelength range of ca. 300-800 nm (Fig. 2b, Supporting Information Fig. S6b, S7b). As shown in Fig. 2b, the devices based on both as-cast and added 0.75% DIO blend films all show a high maximum EQE value over 75%, indicating efficient photon-harvesting and charge collection of PSCs. Compared with the devices based on as-cast film, the EQE spectra show a red-shift and a higher value from 300 to 570 nm and 730 to 800 nm for the devices after adding 0.75% DIO, which can be attributed to the broader absorption spectrum of 0.75% DIO added PTZP:IDIC blend film (Supporting Information Fig. S8), and the higher EQE value matches well with the higher J_{sc} values. The integral J_{sc} calculated from the EQE curves were quite consistent with the measured J_{sc} within 5% error.

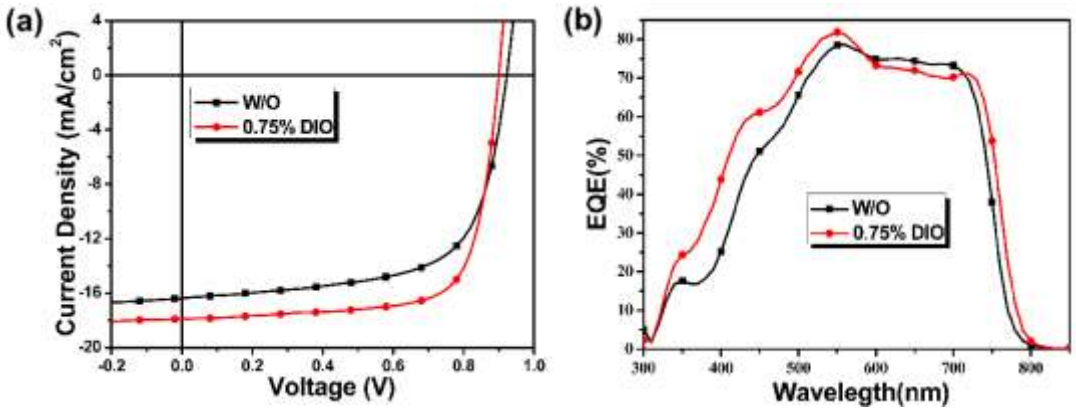

Fig. 2. (a) *J*-*V* curves and (b) EQE spectra of the PSCs based on PTZP:IDIC.

Table 1. Photovoltaic performance of the PSCs based on PTZP:IDIC (1:1.5, w/w) without or with additive under the illumination of AM 1.5 G, 100 mW cm^{-2}.

Additive	V_{oc} (V)	J_{sc}[a)] (mA/cm^2)	FF (%)	PCE[b)] (%)
w/o	0.92	16.4 (15.8)	65.5	9.9 (9.8)
0.75% DIO	0.90	17.9 (17.0)	73.3	11.8 (11.6)

[a)] Values calculated from EQE in brackets. [b)] The average PCE based on 20 devices are shown in brackets.

The charge generation and extraction of PSCs was investigated by measuring the photocurrent density (J_{ph}) versus the effective voltage (V_{eff}).[59] As shown in Fig. 3a, J_{ph} reaches saturation (17.3 mA cm^{-2} and 18.5 mA cm^{-2} for the devices with the as-cast and 0.75% added DIO films) at $V_{eff} \geqslant 2$ V, suggesting that the electrodes extracted all of the photogenerated charge carriers. The J_{ph}/J_{sat} values under short-circuit and maximum power points are 94% and 74% for the as-cast devices, 96% and 78% for the devices with 0.75% DIO addition, respectively. The enhanced J_{ph}/J_{sat} value indicated that the PSCs after adding 0.75% DIO get more efficient excition dissociation and charge extraction efficiencies, which is consistent with the higher J_{sc} of the devices with the added 0.75% DIO. The photoluminescence (PL) spectra of the pure PTZP film, IDIC film and PTZP:IDIC blend films with or without 0.75% DIO were measured.[60] As shown in Fig. S9 in the Supporting Information, the PTZP:IDIC blend films demonstrated more than 70% PL quenching in comparison with the PL spectra of these pure PTZP or IDIC. Moreover, the device with added 0.75% DIO shows the

higher PL quenching exceeding 93% compared to the as-cast device. High PL quenching value indicates that the devices possess effective photo-induced charge transfer between PTZP and IDIC, which is consistent with the high J_{sc} values in the devices.

The light intensity dependence of J_{sc} and V_{oc} was measured to study the charge transport and recombination behaviors in the PTZP:IDIC based PSCs.[61] Fig. 3b exhibits the logarithmic plots of J_{sc} as a function of the light intensity, showing the power law dependence of $J_{sc} \propto P^S$ (where P is the incident light intensity and S is an exponential constant).[62] The S value close to 1 for the device suggests a weak bimolecular recombination in the device.[63] The S values were determined to be 1.02 and 1.01 for the as-cast and 0.75% DIO doped devices, respectively. Obviously, the S value for both as-cast and 0.75% DIO added devices approaches 1, indicating that the DIO treatment has a negligible impact on the bimolecular recombination process for this blend system. Fig. 3c shows the logarithmic plots of J_{sc} with the light intensity, and the slope of V_{oc} versus log P at 2 kT/q means that the dominant recombination mechanism is monomolecular or trap-assisted recombination, while when the slope close to 1 kT/q suggests that only bimolecular recombination takes place in PSCs (where q is elementary charge, T is the temperature in Kelvin and k is the Boltzmann constant).[64] As shown in Fig. 3c, the devices after treatment with the added 0.75% DIO (1.16 kT/q) show the smaller slopes in comparison with the as-cast devices (1.35 kT/q), which means that the devices upon adding 0.75% DIO have fewer trap-assisted and/or monomolecular recombination compared to those as-cast devices.

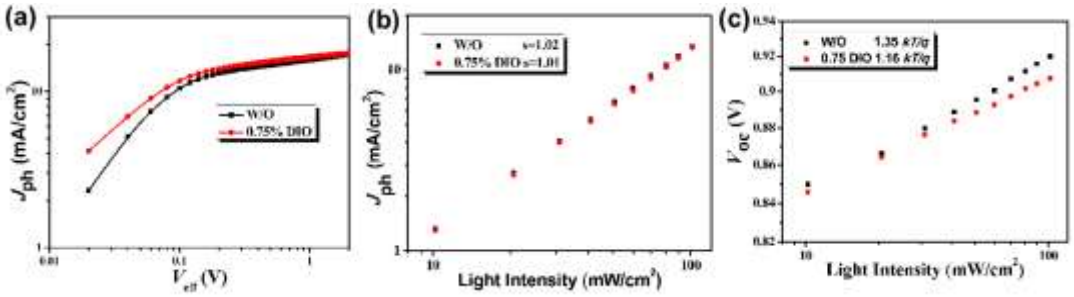

Fig. 3. J_{ph}-V_{eff} characteristics (a), current density (b) and open-circuit voltage (c) *vs* light intensity characteristics.

Grazing incidence X-ray diffraction (GIXD) has been utilized to investigate the microstructures of the neat and blend thin films.[65-66] The two-dimensional GIXD patterns and the corresponding line-cuts for the neat PTZP and the blend films with or without additive are shown in Fig. 4. The PTZP pure film showed obvious lamellar peaks (100) in the in plane (IP) direction at 0.28 $Å^{-1}$ (lamellar d-spacings of 22.36 Å), strong (100) and π-π stacking peak (010) in the out of plane (OOP) direction. For the OOP (010) peak, it was located at 1.72 $Å^{-1}$ (lamellar d-spacings of 22.36 Å). The as-cast blend films produced an additional peak in the (010) π-π stacking peak position in both IP and OOP direction compared to the PTZP pure films, which was owing to the acceptor material IDIC. Upon adding 0.75% DIO, the number of diffraction peaks in both IP and OOP direction are increased and the intensity are enhanced. These characteristics of the increased crystal sizes and preferential face-on orientation lead to improved charge transport in the devices with added 0.75% DIO. The coherence length (L_{100} and L_{010}) was deduced from the full width at half maximum (FWHM) of IP (100) and OOP (010) peaks using the Scherrer equation. The L_{100} and

L_{010} values for the as-cast blend film are 91.61 nm and 28.70 nm, and the correlative values for 0.75% DIO doped blend film are increased to 104.78 nm and 49.24 nm, respectively. These results indicated that the crystallinity of the PTZP was enhanced after adding 0.75% DIO, the more orderly structure is beneficial for charge transport and collection.

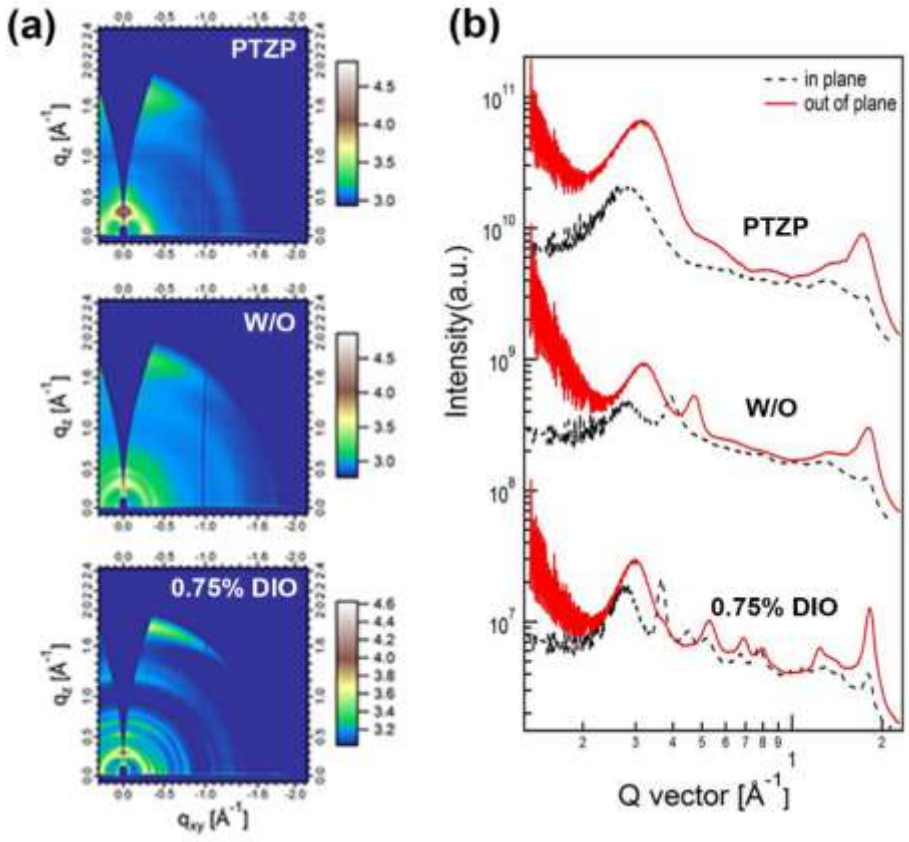

Fig. 4. 2D GIXD diffraction images of the neat PTZP, as-cast blend film and with 0.75% DIO blend film (a); IP (dotted line) and OOP (solid line) X-ray scattering profiles extracted from the 2D GIXD images (b).

To understand the influence of charge carrier mobility on the photovoltaic properties, the hole mobilities of the PTZP pure film and PTZP:IDIC blend films, and the electron mobilities of the PTZP:IDIC blend films were measured by a space

charge limited current (SCLC) method (see Fig. \s and Table S4 in the Supporting Information).[67] The PTZP pure film afforded a fairly high value of 4.01×10^{-3} cm^2 V^{-1} s^{-1}. The hole/electron mobilities (μ_h/μ_e) for the as-cast devices were calculated to be $2.13\times10^{-4}/9.07 \times10^{-5}$ cm^2 V^{-1} s^{-1}. After adding 0.75% DIO, the devices gave a higher and more balanced μ_h/μ_e of $4.51/3.31 \times 10^{-4}$ cm^2 V^{-1} s^{-1}, which is in accordance with the higher J_{sc} and FF of the devices with the added 0.75% DIO.

The phase separation and average domain purity in PTZP:IDIC blend films have been studied by resonant soft X-ray scattering (R-SoXS). A photon energy of 284.2 eV was selected to provide highly enhanced materials contrast. As shown in Fig. 5, the as-cast blend film shows no obvious phase separation. After treatment with the added 0.75% DIO, the blend film exhibits a multi-length scale morphology with a domain size of 92.10 nm, appropriate phase separation can lead to effective exciton dissociation. Moreover, the domain purities for the as-cast and 0.75% DIO blend films are 86% and 100%, respectively. Purer domains can suppress the recombination and result in high-performance PSCs, which agrees with the photovoltaic data of the related devices.[68]

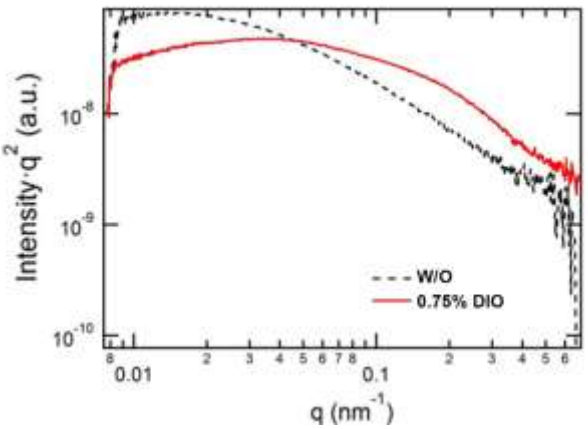

Fig. 5. R-SoXS profiles for PTZP: IDIC blend films.

Atomic force microscopy (AFM) and transmission electron microscopy (TEM) measurements have been carried out to understand the surface and bulk morphologies of the blend films. As shown in Fig. S11 in the Supporting Information, for the AFM images, the as-cast blend film shows a root-mean-square (RMS) roughness of 3.32 nm. After adding 0.75% DIO, the blend film exhibited a slightly lower RMS value of 2.28 nm, which means that the DIO can reduce the surface roughness and optimize the blend morphology effectively. In the TEM images, compared to the as-cast blend film, the blend film upon mixing 0.75% DIO shows more obvious microphase separation and fibrous features, which is in accordance with the result of the R-SoXS test. A better microphase separation is beneficial to charge separation and transport and hence can achieve the higher J_{sc} and FF.

The relationship between the PTZP:IDIC active layer thickness, active area and the photovoltaic performance has been investigated. The *J-V* curves and the corresponding data are shown in Fig. 6a, b and Table 2, and the EQE curves are shown in Figure S12 in the Supporting Information. As shown in Fig. 6a, when the thickness is increased from 70 nm to 200 nm, the V_{oc} puts up a subtle change from 0.91 V to 0.89 V, but the J_{sc} and FF show obvious variation. On the contrary, when the thickness is increased from 75 nm to 100 nm, the J_{sc} value increases from 16.1 mA cm^{-2} to 17.9 mA cm^{-2}, and the FF decreases from 74.5% to 73.3%. When the thickness is increased continuously to 150 nm and 200 nm, the J_{sc} remains at 17.7 mA cm^{-2}, and the FF keeps lowering to 68.2% and 64.5%, respectively. It is observed that with the thickness variation from 70 nm to 200 nm, the PCE of PSCs is stuck at over 10.0%.

Subsequently, the PSCs with different active area have been fabricated, as shown in Fig. 6b. When the active area is increased from 0.04 cm^2 to 0.81 cm^2, the V_{oc} shows no obvious change, while the J_{sc} sharply decreases from 17.9 mA cm^{-2} to 15.9 mA cm^{-2}. Interestingly, when the active area is changed from 0.04 cm^2 to 0.20 cm^2, the FF increases from 73.3% to 74.4%. With the further increase of active area to 0.81 cm^2, the FF is reduced, but the PCE is still as high as 10.2%. The small sensitivity to variation in the active layer thickness and active area suggests that the PTZP:IDIC based PSCs possess a good application prospect.

The storage stability and the thermal tolerance of the PSCs based on PTZP:IDIC with the active layer thickness of 100 nm and active area of 0.04 nm^2 have also been investigated. As shown in Fig. 6c, after over 2000 h of storage in the glove box, the PSCs can still give a high PCE of 10.3%. The heat storage stability of the PSCs has been shown in Fig. 6d, after annealing at 80 °C for 30 h, the PCE is decreased to 9.0%, and it can be held rather steady even when the annealing is continued. After annealing for 64h, the devices still have a high PCE over 8.9%. The above results provided further possible for the application of the PSCs based on PTZP:IDIC

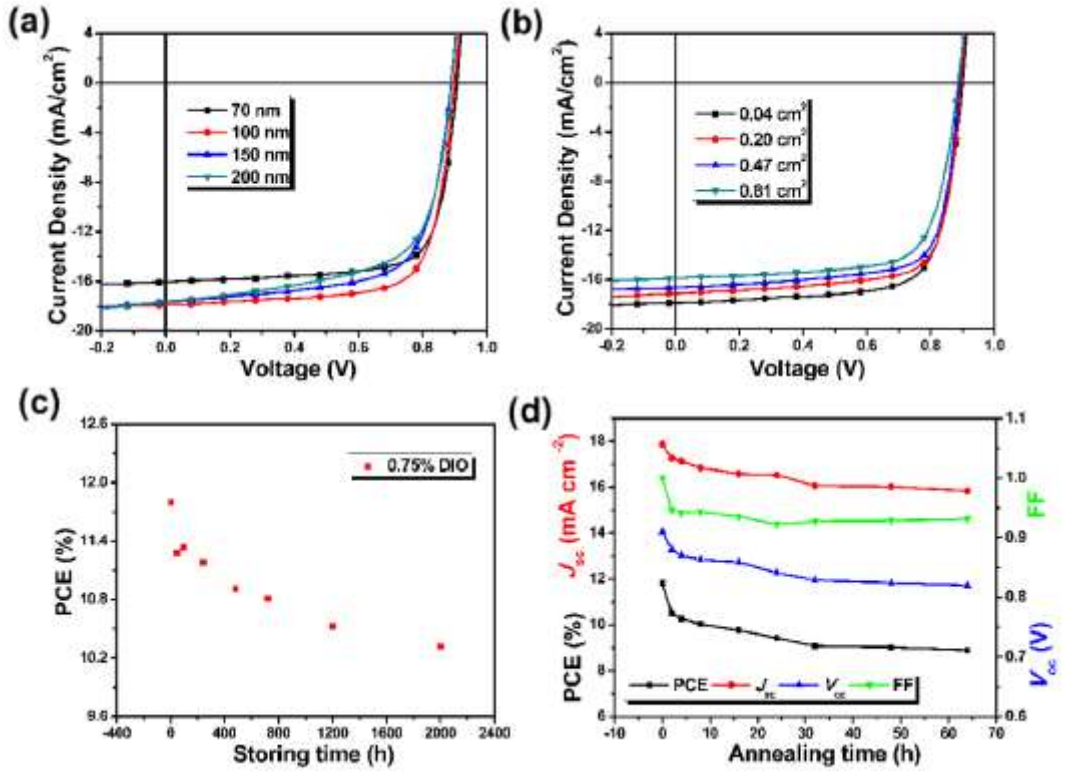

Fig. 6. *J-V* curves of the PSCs based on PTZP**:**IDIC (1:1.5, w/w) with different active layer thickness (a) and different active area (b), storage stability (c) and annealing stability (d) of the PSCs based on PTZP**:**IDIC.

Table 2. Photovoltaic performance of the PSCs based on PTZP:IDIC (1:1.5, w/w) with different active layer thickness and active area under the illumination of AM 1.5 G, 100 mW cm^{-2}.

Thickness (nm)	Area (cm^2)	V_{oc} (V)	J_{sc}[a] (mA cm^{-2})	FF (%)	PCE[b] (%)
75	0.04	0.91	16.1 (15.5)	74.5	10.8 (10.5)
100	0.04	0.90	17.9 (17.0)	73.3	11.8 (11.6)
100	0.20	0.90	17.0 (16.5)	74.4	11.3 (11.1)
100	0.45	0.89	16.7 (15.9)	74.1	10.9 (10.6)
100	0.81	0.89	15.9 (15.5)	72.5	10.2 (10.0)

150	0.04	0.89	17.7 (16.2)	68.2	10.7 (10.5)
200	0.04	0.89	17.7 (16.8)	64.5	10.1 (9.9)

[a)] Values calculated from EQE in parentheses. [b)] The average PCE based on 20 devices are shown in parentheses.

3. Conclusions

In summary, a novel wide-bandgap conjugated polymer (PTZP) was designed, synthesized and characterized. The polymer combining the BDTP and TTz units showed a strong absorption from 300 to 620 nm and a wide-bandgap of 2.01 eV. Non-fullerene BHJ-PSCs were fabricated by using PTZP as the electron donor material and IDIC as the electron acceptor material, a PCE of 9.9% was obtained from the as-cast devices with a high V_{oc} of 0.92 V. After adding 0.75% DIO, the crystallinity of the blend film was enhanced and the morphology of blend film was optimized, so the device showed a high PCE of 11.8% with the sharp increase of J_{sc} and FF. Furthermore, by increasing the active layer thickness to 200 nm or enlarging the device area to 0.81 cm^2, the PSCs based on PTZP:IDIC all showed a high PCE of over 10%. The stability of PSCs has also been studied, after storing the devices in the glove box for 1500 h, the PCE of the devices was still as high as 10.2%. After annealing at 80 °C for 64 h, the PCE was still over 8.0%. The result indicated that the combination of BDTP and TTz units is a successful molecular design strategy to obtain PSCs of high photovoltaic performance, and the PTZP:IDIC based devices has great practical application potential due to the superior PCE and stability.

Acknowledgments

This work was supported by National Natural Science Foundation of China (NSFC) (No. 51503135, 51573120 and 51773142), the Priority Academic Program Development of Jiangsu Higher Education Institutions, Jiangsu Provincial Natural Science Foundation (Grant No. BK20150332). W.-Y.W. thanks the financial support from the Areas of Excellence Scheme, University Grants Committee, HKSAR (AoE/P-03/08), Hong Kong Research Grants Council (PolyU123384/16P), Hong Kong Polytechnic University (1-ZE1C) and the Endowment fund from Ms. Clarea Au (847S). X.G. also acknowledges the support from the Hong Kong Scholars Program. X-ray data was acquired at beamlines 7.3.3 at the Advanced Light Source, which is supported by the Director, Office of Science, Office of Basic Energy Sciences, of the U.S. Department of Energy under Contract No. DE-AC02-05CH11231. The authors thank Dr. Chenhui Zhu at beamline 7.3.3 and Cheng Wang at beamline 11.0.1.2 for assistance with data acquisition.

References

[1] Y. Liu, J. Zhao, Z. Li, C. Mu, W. Ma, H. Hu, K. Jiang, H. Lin, H. Ade, H. Yan, *Nat. Commun.* **2014**, *5*, 5293.

[2] H. Hu, K. Jiang, G. Yang, J. Liu, Z. Li, H. Lin, Y. Liu, J. Zhao, J. Zhang, F. Huang, Y. Qu, W. Ma, H. Yan, *J. Am. Chem. Soc*. **2015**, *137*, 14149.

[3] J. Wan, X. Xu, G. Zhang, Y. Li, K. Feng, Q. Peng, *Energy Environ. Sci.*, **2017**, *10*, 1739.

[4] S. H. Liao, H. J. Jhuo, P. N. Yeh, Y. S. Cheng, Y. L. Li, Y. H. Lee, S. Sharma, S. A. Chen, *Sci. Rep.* **2014**, *4*, 6813.

[5] W. Huang, E. Gann, N. Chandrasekaran, L. Thomsen, S. K. K. Prasad, J. Hodgkiss, D. Kabra, Y.-B. Cheng, C. R. McNeill, *Energy Environ. Sci.*, **2017**, *10*, 1843.

[6] B. Guo, W. Li, X. Guo, X. Meng, W. Ma, M. Zhang, Y. Li, *Adv. Mater.* **2017**, *29*, 1702291.

[7] J. Wang, W. Wang, X. Wang, Y. Wu, Q. Zhang, C. Yan, W. Ma, W. You, X. Zhan, *Adv. Mater.* **2017**, *29*, 1702125.

[8] H. Yao, Y. Chen, Y. Qin, R. Yu, Y. Cui, B. Yang, S. Li, K. Zhang, J. Hou, *Adv. Mater.* **2016**, *28*, 8283.

[9] H. Yao, Y. Cui, R. Yu, B. Gao, H. Zhang, J. Hou, *Angew. Chem. Int. Ed.* **2017**, *56*, 3045.

[10] L. Zuo, J. Yu, X. Shi, F. Lin, W. Tang, A. K. Jen, *Adv. Mater.* **2017**, *29*, 1702547.

[11] W. Zhao, S. Li, H. Yao, S. Zhang, Y. Zhang, B. Yang, J. Hou, *J. Am. Chem. Soc.* **2017**, *139*, 7148.

[12] C. Q. Li, S. Barlow, Z. H. Wang, H. Yan, A. K-Y. Jen, S. R. Marder, X. W. Zhan, *Nat. Rev. Mater.* **2018**, *3*, 18003.

[13] Y. Lin, J. Wang, Z.-G. Zhang, H. Bai, Y. Li, D. Zhu, X. Zhan, *Adv. Mater.*, **2015**, *27*, 1170.

[14] Y. Lin, Q. He, F. Zhao, L. Huo, J. Mai, X. Lu, C.-J. Su, T. Li, J. Wang, J. Zhu, Y. Sun, C. Wang, X. Zhan, *J. Am. Chem. Soc.*, **2016**, *138*, 2973.

[15] Y. Lin, Z.-G. Zhang, H. Bai, J. Wang, Y. Yao, Y. Li, D. Zhu, X. Zhan, *Energy Environ. Sci.*, **2015**, *8*, 610.

[16] B. Kan, H. Feng, X. Wan, F. Liu, X. Ke, Y. Wang, Y. Wang, H. Zhang, C. Li, J. Hou,

Y. Chen, *J. Am. Chem. Soc.*,**2017**, *139*, 4929.

[17] Y. Z. Lin, F. W. Zhao, S. K. K. Prasad, J-D. Chen, W. Z. Cai, Q. Q. Zhang, K. Chen, Y. Wu, W. Ma, F. Gao, J. X. Tang, C. R. Wang, W. You, J. M. Hodgkiss, X. W. Zhan. *Adv. Mater.* **2018**, *30*, 1706363.

[18] J. D. Chen, Y. Q. Li, J. S. Zhu, Q. Q. Zhang, R. P. Xu, C. Li, Y. X. Zhang, Y. S. Huang, X. W. Zhan, W. You, J. X. Tang, *Adv. Mater.* **2018**, *30*, 1706083.

[19] M. Zhang, Y. Sun, X. Guo, C. Cui, Y. He, Y. Li, *Macromolecules* **2011**, *44*, 7625.

[20] Q. Fan, W. Su, X. Guo, Y. Wang, J. Chen, C. Ye, M. Zhang, Y. Li, *J. Mater. Chem. A* **2017**, *5*, 9024.

[21] Y. Firdaus, L. P. Maffei, F. Cruciani, M. A. Müller, S. Liu, S. Lopatin, N. Wehbe, G. O. N. Ndjawa, A. Amassian, F. Laquai, P. M. Beaujuge, *Adv. Energy Mater.*, **2017**, *7*, 1700834.

[22] J. You, L. Dou, K. Yoshimura, T. Kato, K. Ohya, T. Moriarty, K. Emery, C. C. Chen, J. Gao, G. Li, Y. Yang, *Nat. Commun.* **2013**, *4*, 1446.

[23] T. F. Li, S. X. Dai, Z. F. Ke, L. X. Yang, J. Y. Wang, C. Q. Yan, W. Ma, X. W. Zhan, *Adv. Mater.* **2018**, *30*, 1705969.

[24] J. Y. Wang, J. X. Zhang, Y. Q. Xiao, T. Xiao, R. Y. Zhu, C. Q. Yan, Y. Q. Fu, G. G. Lu, X. H. Lu, S. R. Marder, X. W. Zhan, *J. Am. Chem. Soc.* **2018**, DOI: 10.1021/jacs.8b04027.

[25] Y. Li, L. Zhong, B. Gautam, H.-J. Bin, J.-D. Lin, F.-P. Wu, Z. Zhang, Z.-Q. Jiang, Z.-G. Zhang, K. Gundogdu, Y. Li, L.-S. Liao, *Energy Environ. Sci.* **2017**, *10*, 1610.

[26] (a) B. Fan, K. Zhang, X. F. Jiang, L. Ying, F. Huang, Y. Cao, *Adv. Mater.* **2016**, *28*,

1606396. (b) X. Pan, W. Xiong, T. Liu, X. Sun, L. Huo, D. Wei, M. Yu, M. Han, Y. Sun, *J. Mater. Chem. C* **2017**, *5*, 4471.

[27] (a) Y. Cai, L. Huo, Y. Sun, *Adv. Mater.* **2017**, 29, 1605437. (b) Y. Ma, Z. Kang, Q. Zheng, *J. Mater. Chem. A* **2017**, *5*, 1860 (c) X. Pan, L. Huo, Chin. *J. Org. Chem.* **2016**, *36*, 687.

[28] S. Chen, Y. Liu, L. Zhang, P. C.Y. Chow, Z. Wang, G. Zhang, W. Ma, H. Yan, *J.Am. Chem. Soc.* **2017**, *139*, 6298.

[29] Y. Z. Lin, H. J. Fan, Y. F. Li, X. W. Zhan, *Adv. Mater.* **2012**, *24*, 3087.

[30] L. Ye, S. Zhang, L. Huo, M. Zhang, J. Hou, *Acc. Chem. Res.* **2014**, *47*, 1595.

[31] B. Kan, Q. Zhang, M. Li, X. Wan, W. Ni, G. Long, Y. Wang, X. Yang, H. Feng, Y. Chen, *J. Am. Chem. Soc*. **2014**, *136*, 15529.

[32] H. S. Lee, H. G. Song, H. Jung, M. H. Kim, C. Cho, J.-Y. Lee, S. Park, H. J. Son, H.-J. Yun, S.-K. Kwon, Y.-H. Kim, B. Kim, *Macromolecules* **2016**, *49*,7844.

[33] H. Yao, R. Yu, T. J. Shin, H. Zhang, S. Zhang, B. Jang, M. A. Uddin, H. Y. Woo, J. Hou, *Adv. Energy Mater.* **2016**, *6*, 1600742.

[34] H. Hwang, D. H. Sin, C. Kulshreshtha, B. Moon, J. Son, J. Lee, H. G. Kim, J. Shin, T. Joo, K. Cho, *J. Mater. Chem. A* **2017**, *5*, 10269.

[35] B. Kan, Q. Zhang, F. Liu, X. Wan, Y. Wang, W. Ni, X. Yang, M. Zhang, H. Zhang, T. P. Russell, Y. Chen, *Chem. Mater.* **2015**, *27*, 8414.

[36] S. R. Bheemireddy, M. P. Hautzinger, T. Li, B. Lee, K. N. Plunkett, *J. Am. Chem. Soc*. **2017**, *139*, 5801.

[37] C.-Y. Kuo, W. Nie, H. Tsai, H.-J. Yen, A. D. Mohite, G. Gupta, A. M. Dattelbaum,

D. J. William, K. C. Cha, Y. Yang, L. Wang, H.-L. Wang, *Macromolecules* **2014**, *47*, 1008.

[38] L. Huo, J. Hou, S. Zhang, H.-Y. Chen, Y. Yang, *Angew. Chem. Int. Ed*. **2010**, *122*, 1542.

[39] X. Zhu, J. Fang, K. Lu, J. Zhang, L. Zhu, Y. Zhao, Z. Shuai, Z. Wei, *Chem. Mater.* **2014**, *26*, 6947.

[40] P. Zhou, Z.-G. Zhang, Y. Li, X. Chen, J. Qin, *Chem. Mater.* **2014**, *26*, 3495.

[41] T. E. Kang, H.-H. Cho, H. j. Kim, W. Lee, H. Kang, B. J. Kim, *Macromolecules* **2013**, *46*, 6806.

[42] H.-S. Chung, W.-H. Lee, C. E. Song, Y. Shin, J. Kim, S. K. Lee, W. S. Shin, S.-J. Moon, I.-N. Kang, *Macromolecules* **2014**, *47*, 97.

[43] W. Su, Q. Fan, X. Guo, X. Meng, Z. Bi, W. Ma, M. Zhang, Y. Li, *Nano Energy* **2017**, *38*, 510.

[44] M. Zhang , Y. Gu , X. Guo , F. Liu , S. Zhang , L. Huo, T. P. Russell, J. Hou, *Adv. Mater.* **2013**, *25*, 4944.

[45] G. Li, X. Gong, J. Zhang, Y. Liu, S. Feng, C. Li, Z. Bo, *ACS Appl. Mater. Interfaces* **2016**, *8*, 3686.

[46] L. Dou, J. Gao, E. Richard, J. You, C. C. Chen, K. C. Cha, Y. He, G. Li, Y. Yang, *J. Am. Chem. Soc*. **2012**, *134*, 10071.

[47] J.-M. Jiang, H.-K. Lin, Y.-C. Lin, H.-C. Chen, S.-C. Lan, C.-K. Chang, K.-H. Wei, *Macromolecules* **2014**, *47*, 70.

[48] Y. Wang, F. Yang, Y. Liu, R. Peng, S. Chen, Z. Ge, *Macromolecules* **2013**, *46*,

1368.

[49] J. Du, A. Fortney, K. E. Washington, M. C. Biewer, T. Kowalewski, M. C. Stefan, *J. Mater. Chem. A* **2017**, *5*, 15591.

[50] P. Huang, J. Du, M. C. Biewer, M. C. Stefan, *J. Mater. Chem. A* **2015**, *3*, 6244.

[51] B. Guo, X. Guo, W. Li, X. Meng, W. Ma, M. Zhang, Y. Li, *J. Mater. Chem. A* **2016**, *4*, 13251.

[52] L. Huo, X. Guo, S. Zhang, Y. Li, J. Hou, *Macromolecules* **2011**, *44*, 4035.

[53] M. J. Zhang, X. Guo, X. Wang, H. Wang, Y. Li, *Chem. Mater*. **2011**, *23*, 4264.

[54] P. Z. Guo, G. P. Luo, Q Su, J.F. Li, P. Zhang, J. F. Tong, C. Y. Yang, Y. J. Xia, H. B. Wu, *ACS Appl. Mater. Interfaces* **2017**, *9*, 10937.

[55] P. Z. Guo, J. B. Sun, S. Sun, J. F. Li, J. F. Tong, C. Zhao, L. J. Zhu, P. Zhang, C. Y. Yang, Y. J. Xia, *RSC Adv.* **2017**, *7*, 22845.

[56] P. L. Gao, J. F. Tong, P. Z. Guo, J. F. Li, N. N. Wang, C. Li, A. Y. Ma, P. Zhang, C. L. Wang, Y. J. Xia, *J. Polym. Sci., Part A: Polym. Chem.* **2018**, *56*, 85.

[57] J. F. Tong, J. F. Li, P. Zhang, X. Y. Ma, M. Wang, L. L. An, J. B. Sun, P. Z. Guo, C. Y. Yang, Y. J. Xia, *Polymer* **2017**, *121*, 183.

[58] I. Osaka, R. Zhang, G. Sauve´, D.-M. Smilgies, T. Kowalewski, R. D. McCullough, *J. Am. Chem. Soc.* **2009**, *131*, 2521.

[59] J. Wan, X. Xu, G. Zhang, Y. Li, K. Feng, Q. Peng, *Energy Environ. Sci.* **2017**, *10*, 1739.

[60] L. Nian, K. Gao, Y. Jiang, Q. Rong, X. Hu, D. Yuan, F. Liu, X. Peng, T. P. Russell, G. Zhou, *Adv. Mater.*, **2017**, *29*, 1700616.

[61] Y. Deng, J. Liu, J. Wang, L. Liu, W. Li, H. Tian, X. Zhang, Z. Xie, Y. Geng, F. Wang, *Adv. Mater*. **2014**, *26*, 471.

[62] H. G. Song, Y. J. Kim, J. S. Lee, Y.-H. Kim, C. E. Park, S.-K. Kwon, *ACS Appl. Mater. Interfaces* **2018**, *8*, 34353.

[63] X. Ma, F. Zhang, Q. An, Q. Sun, M. Zhang, J. Miao, Z. Hu, J. Zhang, *J. Mater. Chem. A* **2017**, *5*, 13145.

[64] S. R. Cowan, A. Roy, A. J. Heeger, *Phys. Rev. B* **2010**, *82*, 245207.

[65] H. Bin, L. Xiao, Y. Liu, P. Shen, Y. Li, *J. Polym. Sci. Polym. Chem.* **2014**, *52*, 1929.

[66] X. Guo, M. Zhang, C. Cui, J. Hou, Y. Li, *ACS Appl. Mater. Interfaces,* **2014**, *6*, 8190.

[67] T. Yu, X. Xu, G. Zhang, J. Wan, Y. Li, Q. Peng, *Adv. Funct. Mater.* **2017**, *27*, 1701491.

[68] P. Muller-Buschbaum, *Adv. Mater.* **2014**, *26*, 7692.

The table of contents entry

A novel wide bandgap polymer PTZP with E_g^{opt} of 2.01 eV has been designed and synthesized. PSCs based on PTZP exhibited high PCE of 11.8%. PCE over 10% with active layer thickness of 200 nm or area of 0.81 cm^2. These reveal that PTZP will be a promising conjugated polymer for the fabrication of efficient large area PSCs.

Keywords: non-fullerene polymer solar cells, alkylphenyl-substituted benzo[1,2-*b*:4,5-*b'*]dithiophene, thiazolo[5,4-*d*]thiazole, power conversion efficiency.

Wide-bandgap polymer based on alkylphenyl-substituted benzo[1,2-*b*:4,5-*b'*]dithiophene unit with high power conversion efficiency of over 11%

Xia Guo, Wanbin Li, Huan Guo, Bing Guo, Jingnan Wu, Wei Ma, Maojie Zhang*, Wai-Yeung Wong*